



OIST

OKINAWA INSTITUTE OF SCIENCE AND TECHNOLOGY GRADUATE UNIVERSITY
沖縄科学技術大学院大学

Single degree of freedom everting ring linkages with nonorientable topology

Author	Johannes Schonke, Eliot Fried
journal or publication title	Proceedings of the National Academy of Sciences
volume	116
number	1
page range	90-95
year	2018-12-19
Publisher	National Academy of Sciences
Rights	(C) 2019 the Author(s).
Author's flag	publisher
URL	http://id.nii.ac.jp/1394/00000908/

doi: info:doi/10.1073/pnas.1809796115



Single degree of freedom everting ring linkages with nonorientable topology

Johannes Schönke^{a,1} and Eliot Fried^{a,1}

^aMathematics, Mechanics, and Materials Unit, Okinawa Institute of Science and Technology Graduate University, Onna, Okinawa 904-0495, Japan

Edited by Howard A. Stone, Princeton University, Princeton, NJ, and approved November 15, 2018 (received for review June 8, 2018)

Linkages are assemblies of rigid bodies connected through joints. They serve as the basis for force- and movement-managing devices ranging from ordinary pliers to high-precision robotic arms. Aside from planar mechanisms, like the well-known four-bar linkage, only a few linkages with a single internal degree of freedom—meaning that they can change shape in only one way and may thus be easily controlled—have been known to date. Here, we present “Möbius kaleidocycles,” a previously undiscovered class of single-internal degree of freedom ring linkages containing nontrivial examples of spatially underconstrained mechanisms. A Möbius kaleidocycle is made from seven or more identical links joined by revolute hinges. These links dictate a specific twist angle between neighboring hinges, and the hinge orientations induce a nonorientable topology equivalent to the topology of a 3π -twist Möbius band. Apart from having many technological applications, including perhaps the design of organic ring molecules with peculiar electronic properties, Möbius kaleidocycles raise fundamental questions about geometry, topology, and the limitations of mobility for closed loop linkages.

spatial linkages | single degree of freedom | deployable structures | topology | nonorientability

Linkages have been known since antiquity (1, 2). They can be found in nature, as in the powerful jaw mechanism of the parrotfish and the mammalian knee joint (3), in the vertebrate skull (4), in the raptorial appendages of the mantis shrimp (5), and in countless gadgets and machines (6). The latter range from simple manual tools (like bolt cutters) to deployable structures (like umbrellas, foldable camping gear, solar panels for spacecraft, and portable architecture) to intricate components of robots and prosthetic devices.

Designers of deployable structures have considerable interest in adopting notions derived from rigid origami as described, for example, by You (7) or Chen et al. (8). This design principle takes advantage of the folding and unfolding of structures made from flat rigid bodies connected by revolute hinges as exemplified by the famous folding of Miura (9). The resulting constructions belong to the general class of mechanisms made from rigid bodies connected by joints. You and Chen (10) note that all such mechanisms, which they call “motion structures,” combine a small set of fundamental building blocks: scissor-like elements, the Sarrus linkage, the Bennett linkage, and the Bricard linkage. Each of these linkages has one degree of freedom and except for the first, is overconstrained in the sense that it can move, although a simple mobility analysis dictates otherwise.

We present a class of ring linkages (also known as closed loop kinematic chains) that are fundamentally different from all previously known types. These linkages can have an unlimited number (greater than or equal to seven) of identical rigid bodies joined by hinges but still have only a single degree of freedom; an example is shown in Fig. 1. Except for the one with seven hinges, each of these objects is underconstrained, meaning that it has fewer degrees of freedom than a simple mobility analysis would suggest. Since they are rings and share the topology of a 3π -twist Möbius band, these linkages can be called “Möbius

kaleidocycles.” They may serve as building blocks of deployable structures and other machines, but beyond that, they have fascinating properties that raise many questions in mechanical engineering, physics, chemistry, and mathematics. Below, we describe the construction of Möbius kaleidocycles, discuss their distinct features, and sketch potential applications.

Classical and Möbius Kaleidocycles

Classical Kaleidocycles. A classical six-hinged kaleidocycle (K6) is a closed ring of six identical tetrahedra, the opposing edges of which serve as hinges. This object can be identified as the trihedral version of a general linkage invented by Bricard (11) in 1927, which is a closed loop kinematic chain consisting of six links connected by revolute hinges (and is known as a “6R Bricard linkage”). Fig. 2, *Upper* shows a paper model of a conventional K6 and a 3D printed realization of a 6R Bricard linkage that is kinematically equivalent to the paper model. A K6 possesses a single internal degree of freedom manifested by a cyclic everting motion, during which different tetrahedral faces are periodically exposed while a threefold rotational symmetry is preserved. In applications, the single degree of freedom affords controllability and is, therefore, a desirable property. Detailed kinematic analyses of a K6 are in, for example, Arponen et al. (12) and Fowler and Guest (13).

A classical eight-hinged kaleidocycle is made like six-hinged ones but with eight tetrahedra. This object is nevertheless markedly different from its six-hinged counterpart. It has two internal degrees of freedom; in any configuration, it can move in at least two independent directions as shown in Fig. 2, *Lower*.

Significance

Linkages are the basic functional elements of any machine. Known established linkages with a single degree of freedom, which facilitates control, have so far consisted of six or fewer links. We introduce “Möbius kaleidocycles,” a class of single-degree of freedom ring linkages containing nontrivial linkages having less mobility than expected. Möbius kaleidocycles consist of arbitrarily many (but at least seven) identical hinge-joined links and may serve as building blocks in deployable structures, robotics, or chemistry. These linkages are chiral and have a nonorientable topology equivalent to 3π -twist Möbius bands. Other than technological promise, Möbius kaleidocycles pose a myriad of intriguing questions in mechanical engineering, physics, and various areas of mathematics, especially topology.

Author contributions: J.S. and E.F. designed research, performed research, and wrote the paper.

The authors declare no conflict of interest.

This article is a PNAS Direct Submission.

This open access article is distributed under Creative Commons Attribution-NonCommercial-NoDerivatives License 4.0 (CC BY-NC-ND).

¹To whom correspondence may be addressed. Email: johannes.schoenke@oist.jp or eliot.fried@oist.jp.

This article contains supporting information online at www.pnas.org/lookup/suppl/doi:10.1073/pnas.1809796115/-DCSupplemental.

Published online December 19, 2018.



Fig. 1. Rendering of a nine-hinged Möbius kaleidocycle (MK9) made from nine identical links connected through revolute hinges. This ring linkage has only a single degree of freedom manifested by a cyclic everting motion (Movie S1).

This raises a question: how many degrees of freedom does a ring of N tetrahedra linked by N revolute hinges generally have? If the $2N$ tetrahedral corners defining the ring were free points in 3D space, then they would have $3 \cdot 2N$ degrees of freedom. However, the tetrahedral edges constitute constraints forcing pairs of corners to be at a fixed distance. Along with the N hinges, each of the N tetrahedra has four additional such edges, leading to $5N$ constraints. Granted that only internal degrees of freedom are of interest, it is necessary to subtract the six

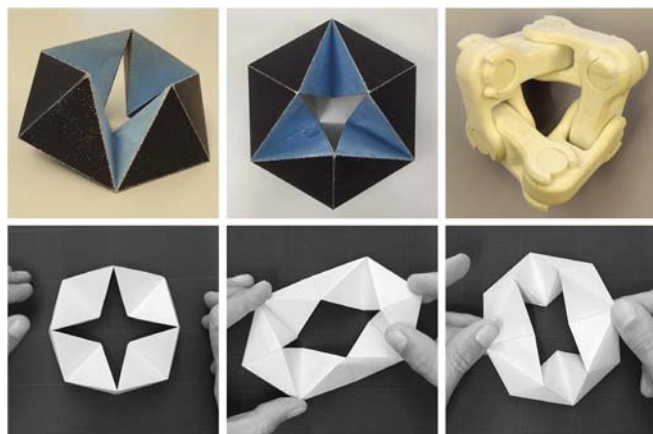


Fig. 2. (Upper) A classical six-hinged kaleidocycle (K6) made from paper (Left and Center) and a 3D-printed 6R Bricard linkage (Right) are kinematically equivalent. Both have a single internal degree of freedom and can undergo a cyclic everting motion. The paper model consists of six tetrahedra with faces that are congruent isosceles triangles, the bases of which serve as hinges; there is a critical hinge length (namely $2/\sqrt{5} \approx 0.8944$ times the length of a leg) above which a K6 cannot undergo a full eversion due to collisions of neighboring tetrahedra. (Lower) A classical eight-hinged paper kaleidocycle made from eight regular tetrahedra. In any configuration, this object can move in at least two independent directions as illustrated.

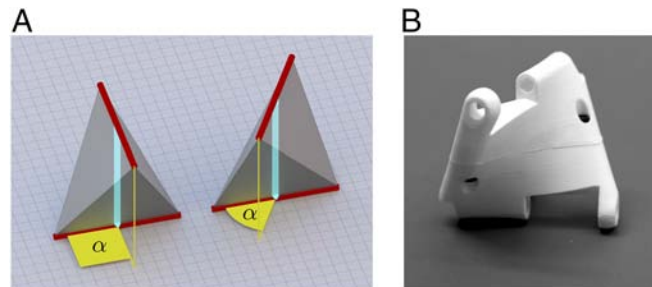


Fig. 3. (A) Convention for defining the twist angle α of a disphenoid. The hinges (red), midaxes (cyan), and twist angles (yellow) are indicated. The tetrahedral midaxis is orthogonal to both hinges. (Left) Regular tetrahedron with orthogonal hinges. (Right) Disphenoid with twist angle $\pi/3$. (B) A single rigid element of the 3D-printed seven-hinged Möbius kaleidocycle (MK7) from Fig. 6 illustrating that the link may have a multitude of shapes granted that the twist angle between the hinges is fixed.

degrees of freedom corresponding to translations and rotations of a rigid body in space. A ring of N tetrahedra should thus have $6N - 5N - 6 = N - 6$ internal degrees of freedom. This raises another question: why does a K6 possess an internal degree of freedom? It transpires that a K6 is a nontrivial example of an overconstrained mechanism. Its high symmetry allows for a hidden degree of freedom.

Möbius Kaleidocycles. The counting argument above shows that classical kaleidocycles made with more than seven tetrahedra usually have several degrees of freedom and thus, move in various ways with no prescribed regular internal motion. What all conventional kaleidocycles share is that the hinges of each tetrahedron are orthogonal. We use generalized tetrahedral shapes, leading to an inherently different class of kaleidocycles. These are disphenoids—or “twisted tetrahedra”—the four faces of which are congruent acute-angled triangles. With this generalization, the two hinges of each tetrahedral link are twisted by a necessarily acute “twist angle” α as illustrated in Fig. 3.

For a chain of identically twisted tetrahedra, there is a natural definition of orientation that allows the chain to be viewed as a twisted band with two “edges” and two “sides.” Each hinge is identified with a vector originating at one of its ends and pointing to the other end. The orientations of two consecutive hinge vectors shared by a tetrahedron are chosen so that the angle between them is the twist angle. The two edges of the twisted band are given by the line segments connecting either the origins (one edge) or the endpoints (the other edge) of the hinge vectors as illustrated in Fig. 4. With this notion of orientation, the closure of the chain induces a topology. The chain can be

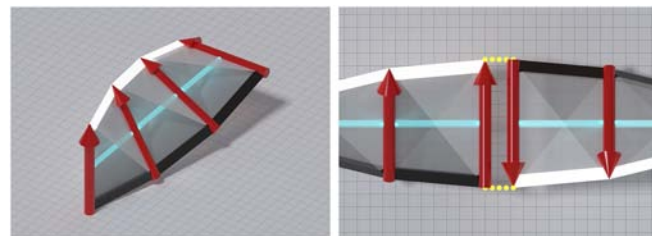


Fig. 4. (Left) Convention for the orientation of a chain of twisted tetrahedra. Each hinge is associated with a vector (red). The line segments between all terminal points of the hinge vectors define the two edges (black and white) of the chain, which can then be viewed as a twisted band. (Right) Closing the chain with the initial and final hinge vectors antiparallel gives a nonorientable ring with a single edge and a topology equivalent to a Möbius band. Each Möbius kaleidocycle is constructed this way.

Table 1. Critical twist angle α_c and total twist angle $N\alpha_c$ for a ring of N twisted tetrahedra

N	α_c/π	$N\alpha_c/\pi$
7	0.4046	2.8319
8	0.3443	2.7541
9	0.3010	2.7091
10	0.2680	2.6800
11	0.2418	2.6598
12	0.2204	2.6452
15	0.1746	2.6189
21	0.1237	2.5974
33	0.0783	2.5847

closed in two ways depending on how the terminal hinges are brought together: the corresponding vectors are either parallel and the closed band is orientable or antiparallel and the band is nonorientable. Hereafter, we consider the nonorientable case. Each such ring is topologically equivalent to a Möbius band.

There is an N -dependent critical twist angle α_c , below which it is impossible to close a chain of $N \geq 7$ identical twisted tetrahedra into a ring in the nonorientable way. More surprisingly, for $\alpha = \alpha_c$, all $N - 6$ degrees of freedom that the ring hypothetically possesses collapse to a single degree of freedom. Each ring formed in this way has the topology of a 3π -twist Möbius band (a shape familiar in stylized form as the recycling symbol), and it seems reasonable to call it a Möbius kaleidocycle. It is also convenient to denote a Möbius kaleidocycle with $N \geq 7$ hinges by MKN and to call the class of linkages consisting of all MKN the Möbius kaleidocycles. In contrast to the K6, each MKN comes in left- and right-handed versions and is, therefore, chiral.

Critical Twist Angle. To show that there is a critical twist angle α_c below which a chain cannot be closed, we need a description for a ring of N rigid bodies, each of which is connected to its neighbors by hinges. Based on concepts laid out by Denavit and Hartenberg (14), we follow the treatment of Bates et al. (ref. 15, pp. 75–76) and describe the hinge orientations of the ring as unit vectors subject to constraints requiring that neighboring hinges have a specified twist angle α and that the ring closes in the nonorientable way. This results in a system of coupled quadratic equations with a real solution set that determines all possible configurations of the ring. To obtain the critical twist angle α_c for a given N , we find solutions of the system for incrementally smaller values of α . Eventually, we reach α_c , below which no real solution exists. Geometrically, this corresponds to a chain that cannot be closed. In *SI Appendix, section 1*, we present the full mathematical description, discuss different solution methods, and detail how we determine α_c . The critical twist angle α_c and the total twist angle $N\alpha_c$ for selected values of $N \geq 7$ are in Table 1.

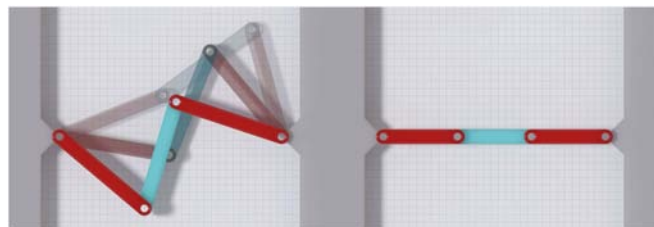


Fig. 5. Example of a trivial planar underconstrained mechanism. While the mechanism in *Left* has one degree of freedom, the mechanism in *Right* cannot move despite having the same number of constraints as the one in *Left*. For this reason, the mechanism in *Right* is designated as underconstrained.

Single Degree of Freedom. One way to confirm that Möbius kaleidocycles have only a single degree of freedom is to show that the real solution set of the system is 1D, corresponding to a curve in the space of all hinge orientations. The algorithm for this is explained in detail in *SI Appendix, section 1*.

A different approach involves viewing kaleidocycles as assemblies of bars and pin joints and performing a kinematic analysis based on Calladine’s generalization of Maxwell’s rule for the stiffness of frames as presented by Pellegrino and Calladine (16). The idea is nicely illustrated with a simple example involving a chain of three bars, where the end joints are connected to the foundation as shown in Fig. 5. If the distance between the foundation joints is less than the sum of the bar lengths, we have a finite mechanism that can move (Fig. 5, *Left*). However, if the distance between the foundation joints equals the sum of the bar lengths, this finite mechanism disappears, and two infinitesimal mechanisms emerge that can be thought of as small displacements of the two internal joints in the direction orthogonal to the bars (Fig. 5, *Right*). Furthermore, a state of self-stress is possible, which here corresponds to a tension in the bars. This self-stress stiffens the two infinitesimal mechanisms. In *SI Appendix, section 3* we describe the Maxwell–Calladine analysis for Möbius kaleidocycles in full detail. We find that an MKN has $N - 5$ mechanisms, $N - 6$ of which are infinitesimal and can be stiffened by a state of self-stress. The one remaining mechanism is not stiffened and corresponds to the single degree of freedom. This places Möbius kaleidocycles in the class of underconstrained “exceptional” mechanisms. Arponen et al. (17) and Müller (18) used algebraic geometry methods to study other simple mechanisms in that class.

Topology of a 3π -twist Möbius Band. The topology of a Möbius kaleidocycle can be characterized by the linking number Lk , namely the number of times that the edge (as defined in Fig. 4) winds around the closed chain of midaxes (cyan in Fig. 4). In an extensive search for real solutions of the system, each time with a random initial guess, we exclusively find $Lk = 3$ corresponding to a 3π -twist Möbius band. The associated procedure is detailed in *SI Appendix, section 1*.

Seven- and Nine-Hinged Möbius Kaleidocycles. We discuss two representative Möbius kaleidocycle subtypes with very distinct features. A paper model of a seven-hinged Möbius kaleidocycle (MK7) is shown in Fig. 6. The motion of this MK7 is notably less regular than the motion of a K6. In any of its configurations, the tetrahedra appear to obstruct one another and thereby, prevent motion. This MK7 can nevertheless undergo a complete eversion (*Movie S2*). The false impression of obstruction arises, because the hinge lengths of the tetrahedra are maximized for the particular design shown. The hinge length is an independent geometric design parameter that specifies the size of the tetrahedra. The constraint forbidding collisions of the tetrahedra during the motion limits the hinge length as in the case of

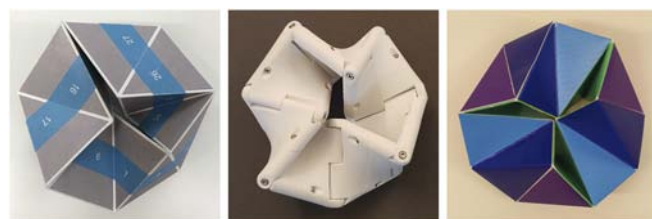


Fig. 6. (*Left and Center*) Paper and 3D-printed seven-hinged Möbius kaleidocycles (MK7). (*Right*) Paper nine-hinged Möbius kaleidocycle (MK9) (*Movies S2–S5*). Interactive visualizations and paper templates for Möbius kaleidocycles are provided online (19).

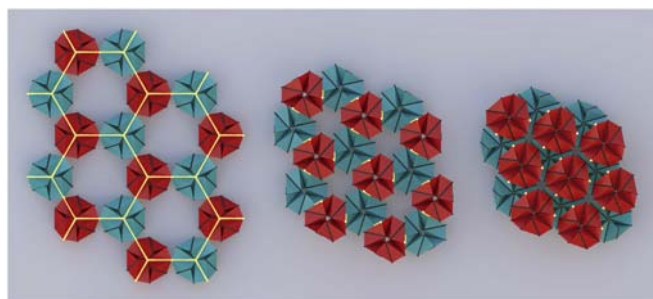


Fig. 7. Rendering of a deployable structure made from nine-hinged Möbius kaleidocycles (MK9). Each MK9 is connected through extended hinges (yellow) to three other MK9 with opposite chirality (distinguished with red and blue) to form a hexagonal lattice. If the MK9 performs the everting motion, a contraction from the extended state (*Left*) to a contracted state (*Center and Right*) occurs.

the K6. This leads to the existence of a maximum hinge length for every MKN . If the hinges for the MK7 paper design in Fig. 6 were any longer, then neighboring tetrahedra would collide in certain phases of the eversion.

An MK9 shares the threefold rotational symmetry of the K6, as shown in Fig. 6, and thus, it differs intrinsically from an MK7. If N is divisible by three, then an MKN also has that same symmetry. Due to its symmetry, the motion of an MK9 is much more regular than that of an MK7 as [Movies S1, S4, and S5](#) show. The hinge length for the paper MK9 in Fig. 6 and [Movie S4](#) is again maximal; were the hinges any longer, triples of tetrahedra would collide in the center during any attempted eversion.

Deployable Structures from Möbius Kaleidocycles. Möbius kaleidocycles can be connected to make deployable structures. To illustrate this, we combine six MK9 to form a hexagonal ring as shown in Fig. 7. Adjacent MK9 in this elementary unit cell have opposite chirality and are connected through a common hinge. The hexagonal elementary cell defined in this way can then be extended to form a 2D lattice. As all MK9 undergo an everting motion, one chiral group of MK9 moves in front of the other group, and the lattice contracts. The two chiral groups form individual triangular lattices that are always parallel, such as is evident from Fig. 7. The extended and contracted configurations of a prototypical hexagonal ring built from six 3D-printed MK9 are shown in Fig. 8. Another idea for a deployable structure is a tetrahedron formed by four MK9, where in each MK9, three symmetric hinges are extended to

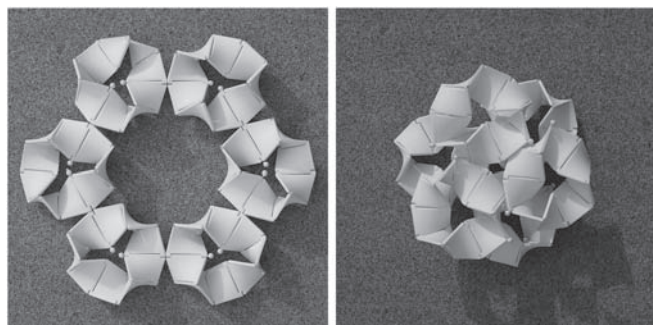


Fig. 8. Photograph of a deployable structure made from six 3D-printed nine-hinged Möbius kaleidocycles (MK9). Each MK9 is connected to three neighbors with opposite chirality through a common hinge. (*Left*) The extended state. (*Right*) As the MK9 evert, the structure contracts, and three MK9 of the one chirality move vertically relative to their enantiomers.

meet the corresponding hinges of the other MK9 in ball joints positioned at the corners of a tetrahedron.

Energetics. Möbius kaleidocycles subject to internal forces that depend on the current configuration of the cycle show interesting behavior. We attach a torsional spring of stiffness B at each hinge of an MKN , $N \geq 7$, as shown for $N = 7$ in Fig. 9. An analysis of a K6 with various choices for the torsional springs was conducted by Safsten et al. (20). On introducing the joint angle θ_i between the midaxes of the tetrahedra adjacent to hinge $i = 1, \dots, N$, the torsional springs correspond to a potential elastic bending energy E and a relative energy variation V_E during eversion given by

$$E = \frac{B}{2} \sum_{i=1}^N \theta_i^2 \quad \text{and} \quad V_E = \frac{\max(E) - \min(E)}{\text{mean}(E)}; \quad [1]$$

V_E is indicative of the forces necessary to overcome the potential energy barriers. For a K6, V_E is about 0.118, which is a substantial variation. Remarkably, for MK7, V_E drops to $2.57 \cdot 10^{-8}$. Thus, if a K6 and an MK7 were endowed with identical springs, the force needed to induce an eversion of an MK7 would be smaller by a factor of more than 4 million compared with that needed to induce an eversion of a K6. As such, an MK7 has an essentially flat energy landscape and behaves virtually identically with or without springs. From this, we infer that, in an MK7, an intrinsic averaging process efficiently redistributes bending energy between the hinges during eversion. Fig. 9 shows the relative energy variation for a K6 and Möbius kaleidocycles

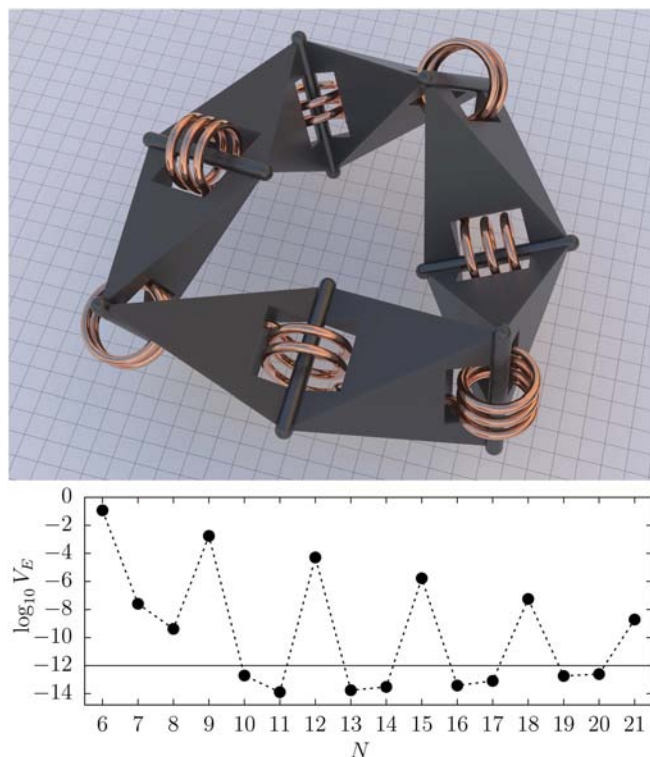


Fig. 9. (*Upper*) Attaching torsional springs of stiffness B to the hinges of a seven-hinged Möbius kaleidocycle (MK7) gives rise to an elastic bending energy E [1]. (*Lower*) The corresponding relative energy variation V_E [1] for a K6 and Möbius kaleidocycles MKN , $N = 7, \dots, 21$. The force exerted during the everting motion of an MK7 is more than 4 million times smaller than for a K6. The solid line at $V_E = 10^{-12}$ indicates the limiting accuracy due to limited floating point precision of the computations; values below 10^{-12} present only an upper bound.

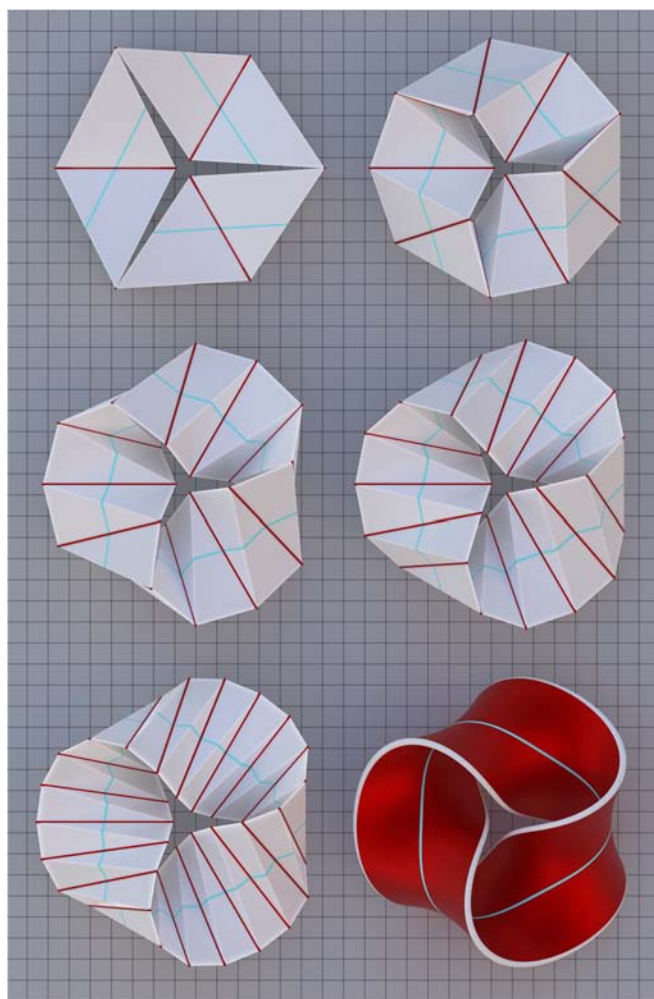


Fig. 10. The six-hinged kaleidocycle (K6) and a sequence of Möbius kaleidocycles MKN with increasing number $N > 7$ of minimally twisted tetrahedra together with the smooth limit surface \mathcal{S} illustrate the limit process $N \rightarrow \infty$. Shown are a K6 (Top Left), MK9 (Top Right), MK12 (Middle Left), MK15 (Middle Right), MK21 (Bottom Left), and the limit surface \mathcal{S} for $N \rightarrow \infty$ (Bottom Right), a 3π -twist Möbius band. The hinges are red, and the limit surface, viewed as a collection of infinitely many hinges, is also red. Note that threefold symmetric rings are chosen only for aesthetic reasons; the limit sequence consists of all natural numbers $N \geq 6$.

up to $N = 21$. It is apparent that V_E for threefold symmetric cycles—namely MKN with N divisible by three—is much greater in comparison with V_E for all other MKN . This makes sense; the aforementioned energy-averaging process cannot be as efficient for threefold symmetric cycles, since three springs have the same tension during any stage of an eversion.

The accurate calculation of V_E hinges on a very precise representation of the evverting motion. Using a Fourier expansion, we construct an explicit time parameterization describing the motion while satisfying the geometric constraints with a relative error of at most $5 \cdot 10^{-14}$ as described in *SI Appendix, section 2*. This parameterization allows us to express E as an explicit function of time and to obtain V_E to extremely high precision. In *SI Appendix, section 4*, we plot the energy evolution for an MK9 and in connection with this, the corresponding input-output relations for the kinematic variables (the joint angles θ_i) in the form of compatibility paths.

Limit Surface and Limit Curve. Since the critical twist angle $\alpha_c < \pi/2$ exists for any ring made from N tetrahedra for $N \geq 7$, it is

valid to consider the limit $N \rightarrow \infty$. From Table 1, it is apparent that α_c and $N\alpha_c$ are strictly decreasing functions of N . As $N \rightarrow \infty$, it appears that α_c tends to zero and that $N\alpha_c$ approaches a positive asymptotic value. For the size of the limiting geometry to be finite, it is also necessary that the limiting length of the tetrahedral midaxis vanishes. Due to the finite size constraint, it follows that the midaxis length must scale with $1/N$ as $N \rightarrow \infty$. In concert with these limits, each individual tetrahedron degenerates to a line segment with the length of the hinges. The limiting object is, therefore, a ruled surface \mathcal{S} defined by those line segments as depicted in Fig. 10. This surface has the topology of a 3π -twist Möbius band formed from a rectangular strip with ends that are “glued” together after three half-turns (in contrast to the most commonly depicted case that arises if the ends are glued after only one half-turn). The threefold rotational symmetry of \mathcal{S} is traceable to the corresponding symmetry of all MKN for which N is divisible by three. Although \mathcal{S} is ruled, we note that it is not developable, because the twist generates a negative Gaussian curvature everywhere on \mathcal{S} .

The smooth closed midline \mathcal{C} , shown in Fig. 11, of \mathcal{S} is a curve defined through the limit of the polygonal chain given by the tetrahedral midaxes defined in Fig. 3. Let $\gamma(\sigma)$ be an arc length parameterization of \mathcal{C} , where $\sigma \in [0, \ell]$ is the arc length. From the construction process leading to the limit, it is clear that \mathcal{C} has a uniform torsion $\tau = \tau_0$. An unanticipated finding from our numerical investigations is that the signed curvature κ of \mathcal{C} is of the sinusoidal form $\kappa(\sigma) = \kappa_0 \sin(3\pi\sigma/\ell)$, where $\kappa_0 > 0$ is constant. We obtain the numerical values $\kappa_0 \approx 13.023/\ell$ and $\tau_0 \approx 8.0941/\ell$. An introduction to signed curvature is in Fenchel (21). Signed curvature and its usefulness is further discussed by Bates and Melko (22), who give explicit constructions of closed curves with constant torsion.

The edge $\partial\mathcal{S}$ of the limiting surface \mathcal{S} is a trefoil knot that winds around the unknot \mathcal{C} as can be inferred from Fig. 11, Bottom Right. The linking number $\text{Lk}(\partial\mathcal{S}, \mathcal{C})$ determined by the Gauss linking integral is a topological invariant that represents the number of times that $\partial\mathcal{S}$ and \mathcal{C} wind around one

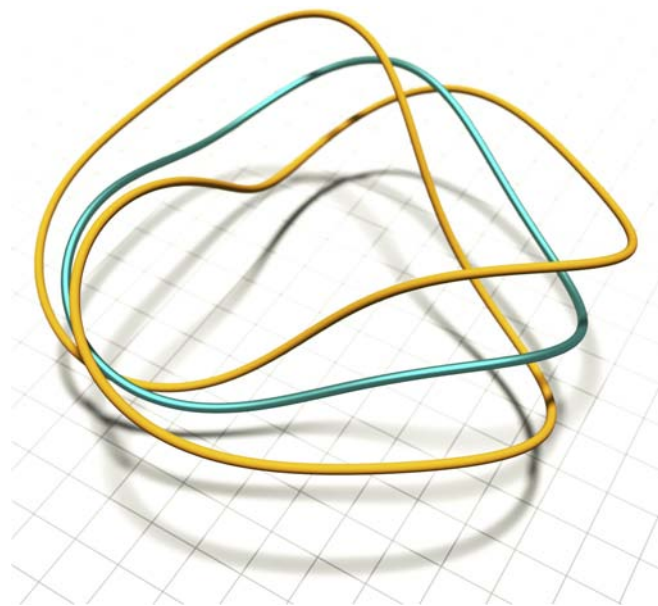


Fig. 11. The midline \mathcal{C} (cyan) and edge $\partial\mathcal{S}$ (yellow) of the limit surface \mathcal{S} (for rulings shorter than those in Fig. 10); \mathcal{C} and $\partial\mathcal{S}$ are smooth and nonself-intersecting and, as indicated by the shadow cast, have threefold rotational symmetry. The trefoil knot $\partial\mathcal{S}$ winds three times around the unknot \mathcal{C} , resulting in a linking number $\text{Lk}(\partial\mathcal{S}, \mathcal{C}) = 3$.

another. Consistent with S being a 3π -twist Möbius band, we find that $\text{Lk}(\partial S, C) = 3$. Establishing a connection to ribbon theory, we identify the twist $\text{Tw}(S)$ of S with the total twist angle in the limit $\lim_{N \rightarrow \infty} N\alpha_c$ (or equivalently, the net torsion $\tau_0 \ell$ of C) divided by 2π to give $\text{Tw}(S) \approx 1.288213$. Following a method by Klenin and Langowski (23), we calculate the writhe $\text{Wr}(C)$ of C to be $\text{Wr}(C) \approx 0.211787$ and establish a variant of Călugăreanu's theorem $\text{Lk}(\partial S, C)/2 = \text{Tw}(S) + \text{Wr}(C)$ connecting the topological quantity Lk to the geometric quantities $\text{Tw}(S)$ and $\text{Wr}(C)$, with the factor $1/2$ being due to the nonorientability of S .

Discussion

We have introduced a class of ring linkages made from rigid bodies joined by revolute hinges. Each of these Möbius kaleidocycles is made from seven or more identical links but has only a single degree of freedom manifested by an everting motion more intricate, by far, than that of a classical six-hinged kaleidocycle (K6). This linkage class forms the basis for applications in many distinct fields. As individual objects, Möbius kaleidocycles may be used as robotic arms or as self-propelling rings that swim through liquids. Due to their highly irregular motions, the smaller linkages without threefold rotational symmetry (e.g., MK7, MK8, MK10, and MK11) seem destined for applications involving mixing and kneading or in light effect machines. We reiterate that there are no limits on the shapes of the links as long as collisions are avoided; moreover, a certain shape design may evoke collisions that intentionally result in only limited motions. The practically flat energy landscape of, for example, an MK7 augmented with torsional springs allows for the design of an openable ring that is equivalent to a straight elastic rod in its open form but in its closed form, undergoes a smooth everting motion without any perceivable counterforce. Aside from the two examples of deployable structures provided here, Möbius

kaleidocycles can be connected rigidly via hinges, ball joints, or other linkages in limitless ways to create new mechanisms.

Synthetic chemistry is another field of potential applications for Möbius kaleidocycles. Building on the seminal contributions of Heilbronner (24), which among other things, showed that Möbius annulenes should exhibit novel electronic properties, Schaller et al. (25) recently synthesized an annulene with a topology of a 3π -twist Möbius band and showed that it is energetically preferred over its classical π -twist counterpart. In that work, a “twist into writhe” strategy is used to produce an annulene with a lower strain. This strategy of reducing twist is completely analogous to the minimal critical twist angle of the topologically equivalent Möbius kaleidocycle. The 3π -twist Möbius band, therefore, appears to possess the topological and geometrical characteristics necessary to minimize a homogeneously distributed twist. We hypothesize that an annulene made from molecular building blocks (equivalent to our tetrahedra) with a twist angle close to the critical angle should exhibit minimal strain.

Finally, many fundamental questions in the fields of kinematics, geometry, and topology are prompted by Möbius kaleidocycles. Do other ring linkages with more than seven elements with only a single degree of freedom exist? Which ring geometries can undergo an everting motion and why? Which topologies are possible? The limit surface and its midline raise questions like the following. Which topologies can a closed, constantly twisted band have? What is the shape of a closed curve with constant nonzero torsion and minimal total curvature?

ACKNOWLEDGMENTS. We thank Michael Grunwald for producing image renderings and 3D-printed models, Gianni Furio Royer-Carfagni and Shizuo Kaji for illuminating discussions, John de Bryun and Gustavo Gioia for feedback on the first draft of this paper, and two anonymous referees for constructive criticism and suggestions. We also acknowledge support from the Okinawa Institute of Science and Technology Graduate University with subsidy funding from the Cabinet Office, Government of Japan.

- Usher AP (1929) *A History of Mechanical Inventions* (McGraw-Hill, New York).
- Paz EB, Ceccarelli M, Otero JE, Sanz JLM (2010) *A Brief Illustrated History of Machines and Mechanisms* (Springer, Dordrecht, The Netherlands).
- Muller M (1996) A novel classification of planar four-bar linkages and its application to the mechanical analysis of animal systems. *Phil Trans R Soc Lond B Biol Sci* 351:689–720.
- Olsen AM, Westneat MW (2016) Linkage mechanisms in the vertebrate skull: Structure and function of three-dimensional, parallel transmission systems. *J Morphol* 277:1570–1583.
- Patek SN, Nowroozi BN, Baio JE, Caldwell RL, Summers AP (2007) Linkage mechanics and power amplification of the mantis shrimp's strike. *J Exp Biol* 210:3677–3688.
- Sclater N, Chironis NP (2007) *Mechanisms and Mechanical Devices Sourcebook* (McGraw-Hill, New York), 4th Ed.
- You Z (2014) Folding structures out of flat materials. *Science* 345:623–624.
- Chen Y, Peng R, You Z (2015) Origami of thick panels. *Science* 349:396–400.
- Miura K (1985) Method of packaging and deployment of large membranes in space. *Inst Space Astronaut Sci Rep* 618:1–9.
- You Z, Chen Y (2012) *Motion Structures* (Spon Press, New York).
- Bricard R (1927) *Leçons De Cinématique*. Tome II, Cinématique Appliquée. (Gauthier-Villars, Paris).
- Arponen T, Piipponen S, Tuomela J (2009) Kinematic analysis of Bricard's mechanism. *Nonlinear Dyn* 56:85–99.
- Fowler P, Guest S (2005) A symmetry analysis of mechanisms in rotating rings of tetrahedra. *Proc R Soc Lond A Math Phys Eng Sci* 461:1829–1846.
- Denavit J, Hartenberg RS (1955) A kinematic notation for lower-pair mechanisms based on matrices. *Trans. ASME J Appl Mech* 22:215–221.
- Bates DJ, Sommese AJ, Hauenstein JD, Wampler CW (2013) *Numerically Solving Polynomial Systems with Bertini* (SIAM, Philadelphia).
- Pellegrino S, Calladine CR (1986) Matrix analysis of statically and kinematically indeterminate frameworks. *Int J Sol Struct* 22:409–428.
- Arponen T, Müller A, Piipponen S, Tuomela J (2014) Kinematical analysis of overconstrained and underconstrained mechanisms by means of computational algebraic geometry. *Meccanica* 49:843–862.
- Müller A (2016) Local kinematic analysis of closed-loop linkages—mobility, singularities, and shakiness. *J Mech Robotics* 8:041013.
- Schönke J (2018) Möbius Kaleidocycle templates and interactive visualizations. Available at hannes.home.oist.jp/kaleidocycles.html. Accessed December 5, 2018.
- Safsten C, Fillmore T, Logan A, Halverson D, Howell L (2016) Analyzing the stability properties of kaleidocycles. *J Appl Mech* 83:051001.
- Fenchel W (1951) On the differential geometry of closed space curves. *Bull Amer Math Soc* 57:44–54.
- Bates LM, Melko OM (2013) On curves of constant torsion I. *J Geom* 104:213–227.
- Klenin K, Langowski J (2000) Computation of writhe in modeling of supercoiled DNA. *Biopolymers* 54:307–317.
- Heilbronner E (1964) Hückel molecular orbitals of möbius-type conformations of annulenes. *Tetrahedron Lett* 5:1923–1928.
- Schaller GR, et al. (2014) Design and synthesis of the first triply twisted Möbius annulene. *Nat Chem* 6:608–613.